Experimental Investigation of Effects of Dwell Angle on Fuel Injection and Diesel Combustion in a High-Speed Optical CR Diesel Engine

Mohammad Reza Herfatmanesh and Hua Zhao

Centre for Advanced Powertrain and Fuels Research, School of Engineering and Design, Brunel University London, UK

ABSTRACT: In order to meet the ever more stringent emission standards, significant efforts have been devoted to the research and development of cleaner internal combustion engines. Diesel combustion and the formation of pollutants are directly influenced by the spatial and temporal distribution of the fuel injected. This study investigated the effects of dwell angle of the split injection on diesel combustion and emissions in a high-speed common rail direct injection optical diesel engine. The fuel injection system was characterised through the measurement of the fuel injection rate and quantity for the tested strategies on a fuel injection test rig. In particular, the interaction between the two injection events was identified. Effects of the split injection dwell angle and the interactions of two consecutive injection events on diesel combustion and exhaust emissions were then investigated in the single cylinder optical engine using the heat release analysis and optical diagnostic techniques. The fuel injection process was illuminated by a high repetition copper vapour laser and recorded synchronously by a high speed video camera. The combustion temperature and soot distribution during the combustion process were measured by a recently developed high speed two-colour system. The results indicated that this injection mode has the potential to improve fuel economy and engine performance while substantially reducing the combustion noise, provided that the injection timings are appropriately selected.

Keywords: diesel engine, injection rate, split injection, dwell angle, emissions

1 INTRODUCTION

Although diesel engines are extremely robust and reliable, capable of producing outstanding torque at low speeds, inherent high levels of regulated and unregulated emissions and combustion noise associated with conventional diesel engines have been the foremost reasons for relatively low market share until the late 1990s. However, recent developments in diesel engine technology, higher fuel prices as well as incentivising tax regimes based on CO_2 emission levels have led to a substantial shift in the automotive market with diesel engines claiming approximately 50% of the European car market [**1**].

Concern over emission of exhaust pollutants has led to the introduction of emissions legislations since the 1960s. In order to meet the ever more stringent emission standards, significant efforts have been devoted to the research and development of cleaner internal combustion (IC) engines. Diesel combustion and the formation of pollutants are directly influenced by the spatial and temporal distribution of the fuel injected. Consequently, numerous research studies have been conducted aimed at more detailed investigation of fuel-air mixing and combustion processes as well as chemical/physical reactions involved in the production of pollutants, in particular nitrogen oxides (NOx) and particulate matter (PM), the two most perilous emissions produced by diesel engines.

The introduction of the common rail (CR) fuel injection system in the 1990s allowed greater control and flexibility on the fuel injection rate, quantity and timing over the entire operating range of diesel engines. The rate of fuel injection and its effect on combustion noise, emission and performance has been extensively investigated since the early days of diesel engines. Nehmer and Reitz [**2**] studied the effect of several injection rate profiles. Their result indicated that the combustion with injectors having slower rate profiles allowed the combustion to continue later in the expansion cycle. Although this resulted in the reduction of soot emissions through improved oxidation process, increase in the fuel consumption was reported.

Zambare and Winterbone [**3**] used an optical engine to investigate the effect of injection rate profile of conventional and two-stage fuel injection equipments (FIE). The results showed that NOx emission was reduced with the latter injection system in comparison to a conventional injection system, though soot emission was higher, particularly at low loads. Koyanagi et al. [**4**] also used an optical engine equipped with a common rail fuel injection system. They compared the effect of fuel injection rate using a conventional solenoid injector and a piezoelectric injector. The results indicated improvements in fuel and air mixing and soot emission due to higher fuel spray momentum caused by faster opening of piezoelectric injectors with a squarer injection rate profile. The fuel economy was also improved due to better fuel atomisation and mixing, though penalties in terms of combustion noise and NOx emission were incurred.

Tanabe et al. [**5**] developed a novel two-rail system comprising of a low and high pressure rail, feeding a single injector. The experiments were conducted on a heavy duty diesel engine whereby the fuel injection rate was controlled by switching between the rails during fuel injection. Their results showed that fuel injection rate shaping resulted in simultaneous reduction of NOx and soot emissions, particularly at mid speed and high loads where control over combustion led to a more constant pressure combustion process similar to an ideal diesel cycle. Although alternative combustion strategies are also capable of simultaneous reduction of NOx and soot emissions, fuel injection rate shaping allows simultaneous reduction of the aforementioned pollutants with no penalty in terms of fuel economy.

The fuel injection pressure in CR fuel injection system is independent of the engine speed; thus, capable of promoting improved fuel evaporation and mixture formation at low speeds and loads. The implementation of such versatile and flexible fuel injection system led to the development of alternative combustion modes including low temperature combustion (LTC) [**6**-**12**], homogeneous charge compression ignition (HCCI) [**8**, **12**-**15**] and premixed charged compression ignition (PCCI) [**16**-**20**] through the application of different injection strategies. The results revealed the potential for simultaneous reduction of NOx and PM emissions through the application of such combustion modes. The initial investigation on using alternative injection strategies were primarily focused on the application of pilot and main injections or split injections with equal fuel demand per injection (50%/50%) [**2**]. The results demonstrated that shorter ignition delay was achieved due to pilot injection, indicating less premixed combustion, lowering the peak heat release rate. Therefore, NOx emission as well as combustion noise was considerably reduced in comparison to conventional diesel combustion. In addition, the effect of post injection on further reduction of soot emission was examined by Han et al. [**21**] and Farrell et al. [**22**]. Their results showed that soot emission was reduced due to improved soot oxidation which was attributed to higher combustion temperature during mixing controlled combustion phase caused by the combustion of fuel injected during post injection. In order to better understand the mixing process, Zhang et al. [**23**] carried out a series of investigations involving detailed analysis of fuel and air mixing process in a constant volume vessel through the application of laser absorption scattering (LAS). They investigated the mixing process using conventional single injection and compared their results with those obtained through split injection strategies 75%/25%, 50%/50% and 25%/75%. It was reported that the 75%/25% split injection strategy resulted in maximum soot reduction for the tested engine operating conditions. This was mainly attributed to improved mixing due to increased in-cylinder turbulence caused by the combustion of fuel injected during second injection.

More recently injection strategies have been investigated with up to 8 injections due to improved capability of modern fuel injection systems [**7**]. Gill and Zhao [**24**] investigated the effect of multiple injection strategy on diesel combustion and emission characteristics using commercially available diesel fuel and biofuels. HCCI combustion was achieved through the use of multiple injection strategies which resulted in the reduction of exhaust emissions. These results were further confirmed through the application of optical diagnostic techniques such as two-colour, chemiluminescence imaging and high speed video imaging. Nevertheless, diesel combustion and the associated mechanisms of pollutant formation are yet to be fully explored and require further investigation in order to meet future emissions legislations. Thus, conventional methods of engine measurement are no longer sufficient for further development of diesel engines. Instead, nonintrusive optical diagnostic techniques have been devised for in-depth analysis of fuel and air mixing.

The objective of this study was to investigate the effect of dwell angle on the combustion performance and emissions through the application of 70%/30% split injection strategy in a single cylinder direct injection high-speed optical diesel engine by means of both conventional heat release analysis and advanced optical diagnostic techniques. During the course of the investigation, it was discovered that there were significant interactions between the two consecutive fuel injection events in the solenoid

CR fuel injector. A fuel injection characterisation rig and fuel bulk modulus measurement device were commissioned and applied to quantify the interaction of two closely coupled fuel injections. Therefore, in the first part of the paper, the principle and application of a fuel injection rate measurement technique are presented. Then the experimental setup and in-cylinder measurement techniques are described. Effects of the split injection dwell angle and the interactions of two consecutive injection events on combustion process and pollutant formation are then presented and discussed.

2 FIE CHARACTERISATION

In this study, a fuel injection rate characterisation rig was commissioned in order to study the effects of multiple injection and alternative diesel fuels on the performance of high pressure fuel injectors.

2.1 Principle of the Fuel Injection Rate Measurement Rig

The evaluation method employed in this study was based on the Zeuch's method presented by Ishikawa et al. [**25**]. The principle of this technique is based on the injection of fuel into a constant volume chamber (CVC) filled with the selected fuel for the measurements, in this case commercially available diesel fuel. Consequently, the pressure inside the chamber increases, this augmentation is proportional to the quantity of fuel injected. Therefore, the rise in pressure (ΔP) can be determined by the following expression as a function of the change in volume (ΔV),

$$\Delta P = k \frac{\Delta V}{V} \qquad (1)$$

Where k Bulk modulus of fuel

V Total volume of the CVC

The fuel injection rate can be determined by differentiating Equation 1 with respect to time (t) as depicted below,

$$\frac{dV}{dt} = \frac{V}{k} \times \frac{dP}{dt} \qquad (2)$$

In the case of a single injection, fuel quantity and injection duration as a function of injection pulse width could be measured through the application of this technique. In addition, interference between injections could also be identified for split or multiple injections, whereby substantial variations in the quantity and rate of fuel injection could be experienced.

However, the bulk modulus of a fluid changes with pressure, thus accurate measurement of fuel injection rate requires evaluation of bulk modulus as a function of the CVC pressure. The bulk modulus of commercially available diesel fuel was experimentally evaluated using a test rig designed and manufactured at Brunel University, which allowed bulk modulus measurements up to 600 bar. The bulk modulus of commercially available diesel fuel as a function of pressure is shown in Figure 1. The measurement at a given pressure reading was repeated twenty times ensuring the repeatability of the results.

2.2 Experimental Setup of the Fuel Injection Rate Measurement Rig

A CVC, of approximately 50 cm^3, equipped with three pressure sensors was employed in this study. The first sensor, Kistler 4043A50 piezo-resistive absolute pressure transducer, measured the pressure inside the chamber prior to fuel injection (i.e. back pressure) while the second and the third sensors, Kistler 701A piezoelectric pressure transducers with high and low sensitivities, were installed for the measurement of small and large fuel quantities (i.e. pilot and main injections) respectively. The piezoelectric pressure transducers were adopted in this setup since their accuracy is often not affected by the size or the volume of the quartz, but the geometry and material used, enabling acquisition of accurate data even at absolute pressures ten times higher than their measuring dynamic full scale range.

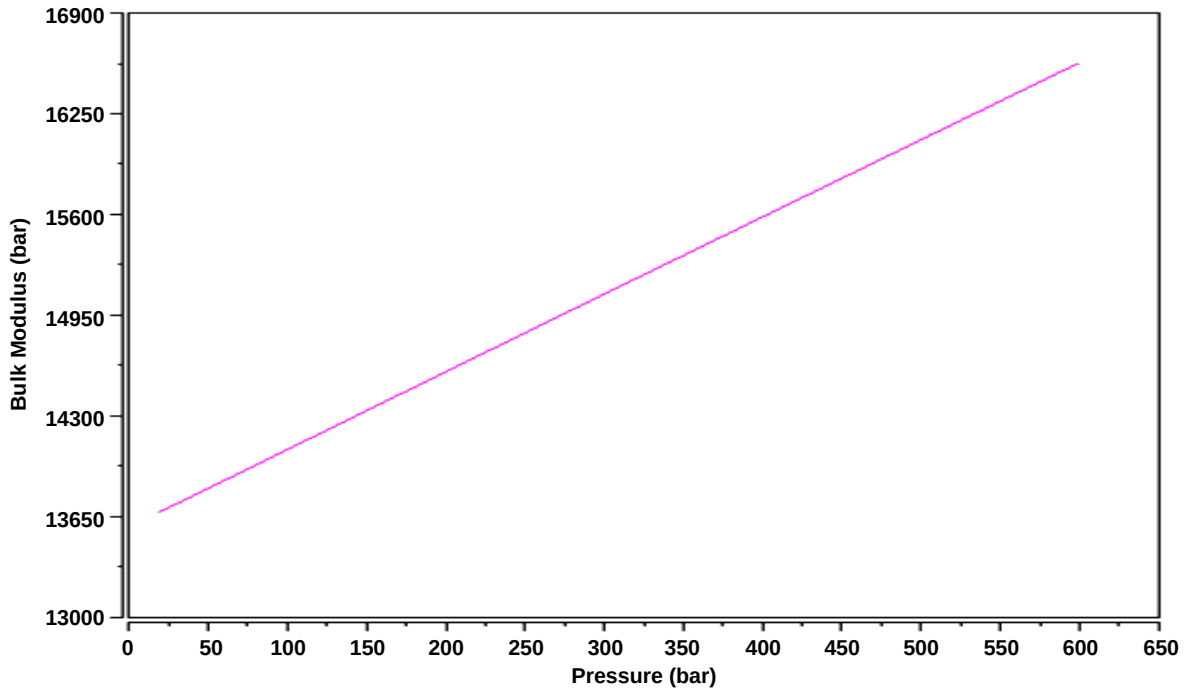

Figure 1. Bulk modulus of diesel fuel

A combination of a pressure relief valve and a solenoid actuator were located on top of the CVC. A schematic diagram of the experimental setup employed in this study is depicted in Figure 2. A high pressure direct acting coaxial solenoid valve was positioned directly on top of the CVC. A Swagelok R series proportional relief valve was utilised in order to regulate the back pressure. In addition, a high precision positive displacement fuel flow meter, ONO SOKKI FP-200 series, was mounted after the pressure relief valve, measuring the quantity of the fuel injected. The fuel quantities calculated based on the application of the Zeuch's method were further validated by the fuel quantities measured by the flow meter. The fuel injector was positioned horizontally opposite the pressure sensors such that the pressure rise inside the CVC could be accurately measured.

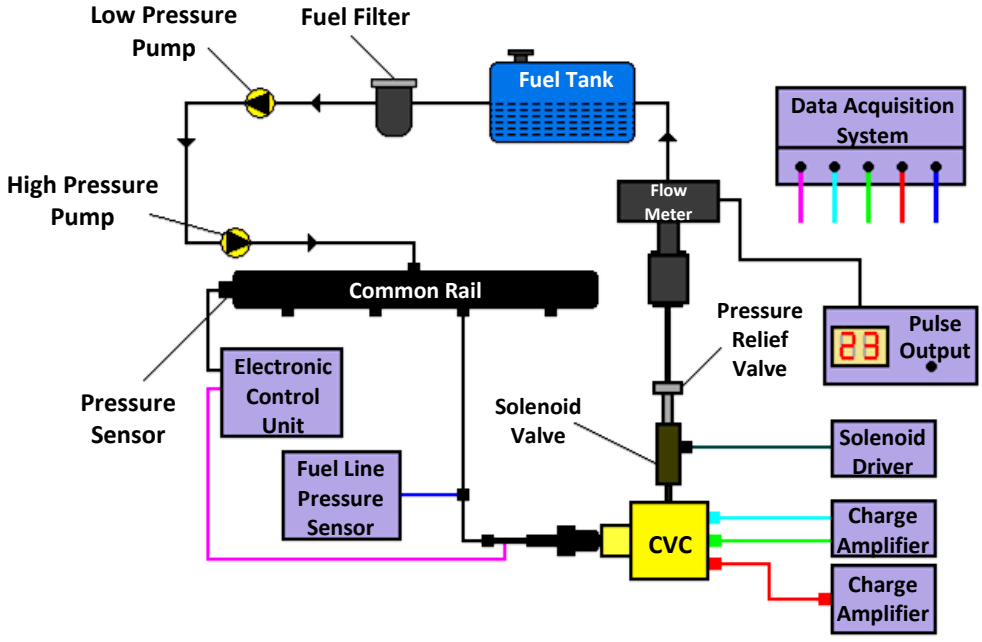

Figure 2. Schematic diagram of fuel injection rate measurement setup

The FIE consisted of a fuel filter, a 12V low pressure pump which drew the filtered fuel from the fuel tank, a first generation Bosch high pressure pump and a Delphi CR fuel injector. The injector utilised in this study was a Delphi multi-hole valve covered orifice (VCO) injector capable of injecting up to 1600 bar. The specifications of the FIE are listed in Table 1.

Table 1. Fuel injection equipment specifications

Injection System	
1st Generation Common Rail System	
Maximum Injection Pressure	1350 bar
Delphi Standard VCO Injector	
Number of Holes	6
Hole Size	0.154 mm
Cone Angle	154°
Flow Rate	0.697 l/min

3 ENGINE AND MEASUREMENT TECHNIQUES

All experimental testing in this study was carried out in a single cylinder high-speed optical engine equipped with a production cylinder head, designed to be representative of a typical modern high-speed direct injection (HSDI) diesel engine. The engine specifications are depicted in Table 2. The engine consisted of a Ricardo Hydra engine crankcase, extended cylinder block and piston and a standard production Ford 2.0 litre ZSD 420 Duratorq engine cylinder head. The details of the common rail fuel injection system are given in Table 1.

Table 2. Single cylinder optical engine specifications

Ricardo Hydra Single-Cylinder Engine	
Bore	86 mm
Stroke	86 mm
Swept Volume	499 cm^3
Compression Ratio	16:1
Piston Bowl	43.4/11.6 mm
	Re-entrant bowl with flat bottom
Swirl Ratio (Ricardo)	1.4

In this study, a Kistler 6125 piezoelectric pressure transducer was installed in place of the glow plug for in-cylinder pressure measurement and heat release analysis. Optical access was provided by the Bowditch piston design which allowed for the visualisation of the combustion chamber through the axis of the cylinder via a glass window, made from fused silica, mounted in the crown of the piston. An extended piston and cylinder block were required in order to accommodate such an optical configuration which consisted of lower and upper parts with a 45° angled mirror, made of glass with aluminised front surface, between the sections. Therefore, the combustion chamber and cylinder walls can be fully visualised through such an optical arrangement, Figure 3.

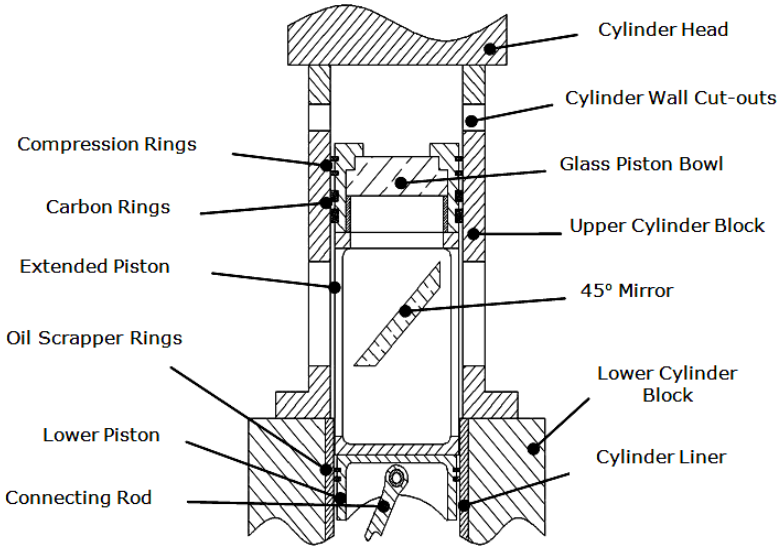

Figure 3. Sectional schematic view of the optical layout

In addition, the upper cylinder block had three rectangular wall cut-outs which can be fitted with glass windows, made of fused silica, for side optical access. Two of these windows were in the same plane allowing laser sheet imaging, Figure 3, while the third window was positioned at 90°, premeditated for imaging and detection purposes.

3.1 Conventional Measurements

For the injection strategies studied, in-cylinder pressure data from 20 consecutive engine cycles was recorded from which the ensemble-averaged heat release rate was calculated. In addition, the soot and gaseous exhaust emissions were measured to assess the effect of the studied dwell angles on engine performance and emissions. The gaseous exhaust emissions of CO, CO_2, O_2, uHC and NOx were measured by means of a Horiba MEXA-7170DEGR analyser while the soot emission was measured using an AVL 415 smoke meter.

3.2 High Speed Spray and Combustion Visualisation

High speed video imaging was employed to record colour images of fuel sprays during the injection period and subsequent combustion process, Figure 4.

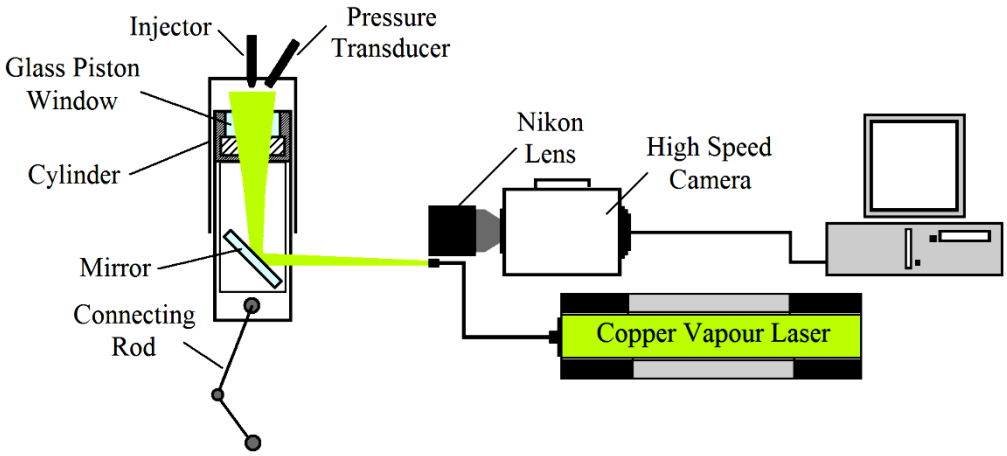

Figure 4. Schematic diagram of direct combustion visualisation setup

In order to visualise the fuel sprays, a high repetition copper vapour Laser was utilised. The output of the laser was delivered to the engine via an optical fibre so that the whole combustion chamber could be illuminated by the divergent laser beam leaving the optical fibre. The short laser pulse of 30ns effectively defined the exposure time of the spray image, which was critical to obtain sharp images of sprays travelling at very high speed. A NAC Memrecam FX6000 high speed colour video camera was used which was equipped with a high speed metal-oxide semiconductor (CMOS) sensor. The high speed camera was set to capture videos at 10,000 frames per second with an image resolution of 512 x 248 pixels. A Nikon 50mm f.1.4 lens was used. A light-emitting diode installed in the field of view of the camera provided the reference signal at top dead centre (TDC) in the high speed video images.

3.3 High Speed Video Two-colour System

The two-colour method is a technique capable of estimating the flame temperature and soot concentration within the combustion chamber of diesel engines [**26**]. This technique is based on the principle of soot luminosity. Diesel combustion is rather luminous due to the radiation of soot particles at elevated temperatures. Therefore, the flame temperature and soot concentration in terms of KL factor can be estimated from the radiation emitted during the combustion process. The blackbody radiation is given by the Plank's law,

$$E_{b,\lambda}(T) = \frac{C_1}{\lambda^5\left[e^{\left(\frac{C_2}{\lambda T}\right)} - 1\right]} \qquad (3)$$

Where $E_{b,\lambda}$ Monochromatic emission power of a blackbody at temperature T

T Temperature

C_1 1st Plank's constant, 3.7510 x 10^{-16} Wm^2

C_2 2nd Plank's constant, 1.4210 μmK

λ Wavelength

Since soot particles do not behave like a blackbody, the radiation emitted by a blackbody and a non-blackbody was linked by introducing the concept of apparent temperature, T_a, which is defined as the temperature at which the radiation emitted by a blackbody is equal to that of a non-blackbody at a temperature T, Equation 4,

$$\varepsilon_\lambda = \frac{e^{\left(\frac{C_2}{\lambda T}\right)} - 1}{e^{\left(\frac{C_2}{\lambda T_a}\right)} - 1} \qquad (4)$$

ε_λ is estimated using an empirical correlation developed by Hottel and Broughton [**27**], Equation 5.

$$\varepsilon_\lambda = 1 - e^{\left(\frac{-KL}{\lambda^\alpha}\right)} \qquad (5)$$

Where K Absorption coefficient proportional to soot density

L Geometrical thickness of the flame along the optical axis of the detection system

α Spectral range constant

The product of K and L is referred to as the KL factor which is proportional to soot concentration, Equation 6,

$$KL = -\lambda^\alpha \ln\left[1 - \left(\frac{e^{\left(\frac{C_2}{\lambda T}\right)} - 1}{e^{\left(\frac{C_2}{\lambda T_a}\right)} - 1}\right)\right] \qquad (6)$$

The soot radiation was measured at two different wavelengths from which two apparent temperatures were calculated. Based on the measured apparent temperatures, flame temperature and soot concentration were estimated using the calibration data obtained with a tungsten lamp. Although this technique has been used in numerous studies due to the simple experimental and calibration setup, there are several sources of uncertainty or errors such as soot deposition on windows, cylinder wall reflections and inadequate sensitivity of the detection system. Therefore care must be taken when interpreting the results, either qualitatively or quantitatively. These factors may lead to experimental errors of 10% [**26**] or even higher depending on the selected wavelengths for measurement. Though, the flame temperature values are less affected [**26**]. Furthermore, most previous two-colour systems were only capable of single shot measurements from different engine cycles, thus suffering from cyclic variations. In order to overcome such a difficulty, a high speed two-colour system was developed. The high speed two-colour measurement system consisted of a NAC Memerecam FX6000 high speed camera and a high repetition image intensifier. Figure 5 shows the experimental setup of the high speed two-colour system. The combustion images were recorded using a standard Nikon 60mm f2.8 lens, in front of which, a custom built optical holder was fabricated to house an image doubler and a set of neutral density and bandpass filters at 550nm and 750nm. The neutral density filters were selected such that the intensity of the combustion images was of similar level at the selected wavelengths.

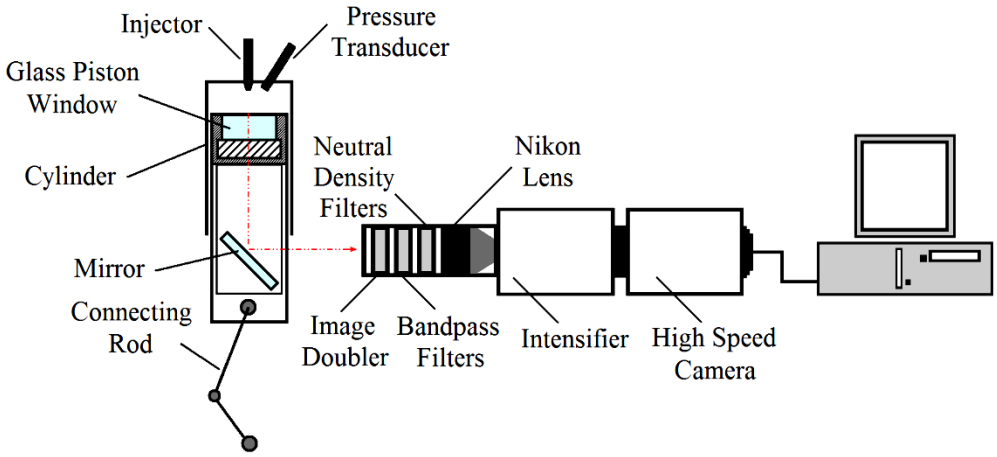

Figure 5. Schematic diagram of high speed two-colour setup

4 ENGINE OPERATING CONDITIONS

The mechanical and thermal stresses the optical components are exposed to during firing cycles are substantial, thus the operating time of optical engines is extremely limited. As a result, both the coolant and the lubricating oil were heated prior to use to ensure reasonable engine temperature was achieved. Thus, problems associated with the cold start were eliminated. In this study injection pulse widths were set to produce 70%/30% split injection strategy with variable dwell angles under part load operating conditions at the engine speed of 1500 rpm, Table 3.

Table 3. Test conditions

Intake Air	100°C Naturally Aspirated (NA), Without EGR
Engine Speed	1500 rpm
Fuel	Commercially Available 49.1 CN Diesel
Fuelling Demand	20 mm^3/cycle
Load	≈ 72% of NA full load, 27.7:1 AFR
Injection Pressure	1200 bar
Piston Bowl	Glass – Pressure, Optical Techniques Metal – Soot, Emissions

The split Injection strategies were selected such that the injection timing of the second injection remained constant at TDC while the injection timing of the first injection was varied. These particular timings were selected amongst a selection of injection timings based on the IMEP values obtained for these strategies. In order to allow comparative analysis of the results, single injection strategies were also performed, serving as the benchmark. The tested strategies are detailed in Table 4.

Table 4. Injection strategies

Strategy	Test No	SOI (CAD ATDC)		Dwell Angle
Single Injection	**A1**	-15		N/A
	A2	-10		
	A3	-5		
	A4	TDC		
		1st	**2nd**	
Split Injection 70%/30%	**F1**	-20	TDC	20
	F2	-15	TDC	15
	F3	-10	TDC	10
	F4	-5	TDC	5

5 RESULTS AND DISCUSSION

5.1 Effect of Dwell Angle on Fuel Injection Quantity

The injection rate profiles for the tested split injection strategies are presented in Figure 6, measured using the Zeuch's method.

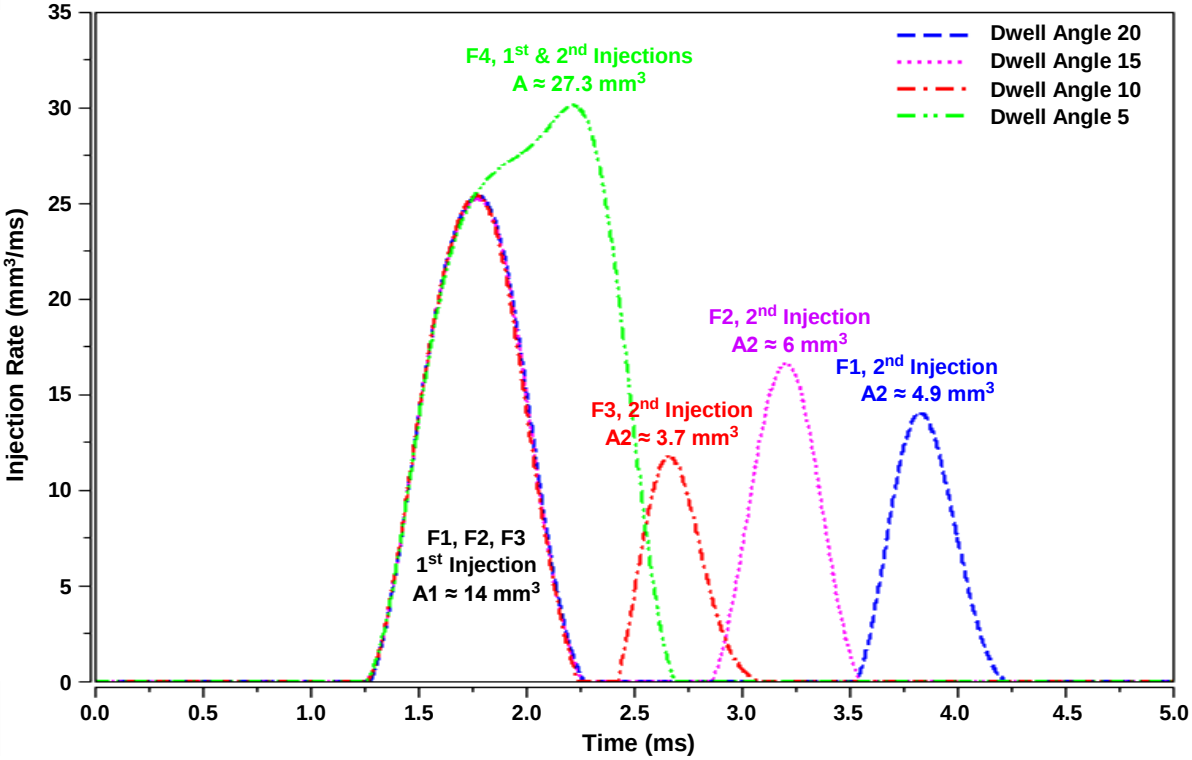

Figure 6. Injection rate profiles for split injection strategies

In the case of 10, 15 and 20 crank angle degree (CAD) dwell angles, the quantity of fuel injected during the first injection remained almost constant, though the quantity of fuel during the second injection varied depending on the dwell angle used. The result for the F4 strategy indicated that 5 CAD dwell angle was not sufficient for the injector to fully close prior to the onset of the second injection, thus almost replicating a single injection. This resulted in the total injected fuel quantity of approximately 27 mm^3 which was substantially higher than the desired quantity of 20 mm^3. These considerable variations in the total fuel quantity injected were mainly attributed to the design limitations of the injector utilised as well as the adverse effect of pressure waves in the high pressure fuel line connecting the injector to the common rail, caused by the first injection. The effects of such inconsistency in fuel delivery on the combustion and emission characteristics were investigated.

5.2 Effect of Dwell Angle and Fuel Quantity on Combustion and Emissions

The calculated and measured data for the injection and combustion characteristics are listed in Table 5. The Injection duration for each individual injection strategy was determined based on the injection rate profiles obtained through the Zeuch's method while the IMEP values and the start of combustion (SOC) timings were calculated from the in-cylinder pressure and heat release rate data respectively. The Ignition delay was also determined from the heat release rate data as the time between the start of the first injection and the onset of the main heat release rate.

The in-cylinder pressure and heat release rate data for the single injection strategies are depicted in Figure 7. The peak in-cylinder pressure decreased as the injection timing was retarded. This was mainly attributed to the late initiation of combustion process during the expansion stroke where the piston was descending after TDC due to retarded fuel injection timing.

The heat release rate curves exhibited a drop due to charge cooling effect shortly after the onset of the fuel injection. Subsequently, the rate of heat release rapidly increased due to the premixed combustion. As given in Table 5, the ignition delay period decreased and the percentage of premixed

Table 5. Injection and combustion characteristics

Test Number	Injection Pressure (bar)	Total Injection Duration (CAD)	IMEP (bar)	Start of Combustion (CAD ATDC)	Ignition Delay (CAD)
A1	1200	5.4	3.06	-6.6	8.4
A2	1200	5.4	3.17	-2.6	7.4
A3	1200	5.4	3.46	2.6	7.6
A4	1200	5.4	4.43	12.6	12.6
F1	1200	7.6	1.544	-9.8	10.2
F2	1200	7.6	3.71	-6.8	8.2
F3	1200	7.6	2.62	-3.4	6.6
F4	1200	7.6	5.74	3.8	8.8

combustion became less as the injection timing was moved towards TDC. The reduction in the amount of heat released from the fast premixed combustion with late injection is compensated for by the faster heat release of combustion in a smaller volume near TDC. As a result, the peak heat release rate remained almost constant for A1, A2 and A3 strategies. However, this trend was not observed for A4 strategy. In this case the ignition delay was much longer and more heat release took place due to premixed combustion, resulting in greater heat release rate. This was mainly due to initiation of combustion during the expansion stroke when the in-cylinder pressure and temperature were lower. Thus, the peak in-cylinder pressure was lowered as the combustion occurred in a larger cylinder volume.

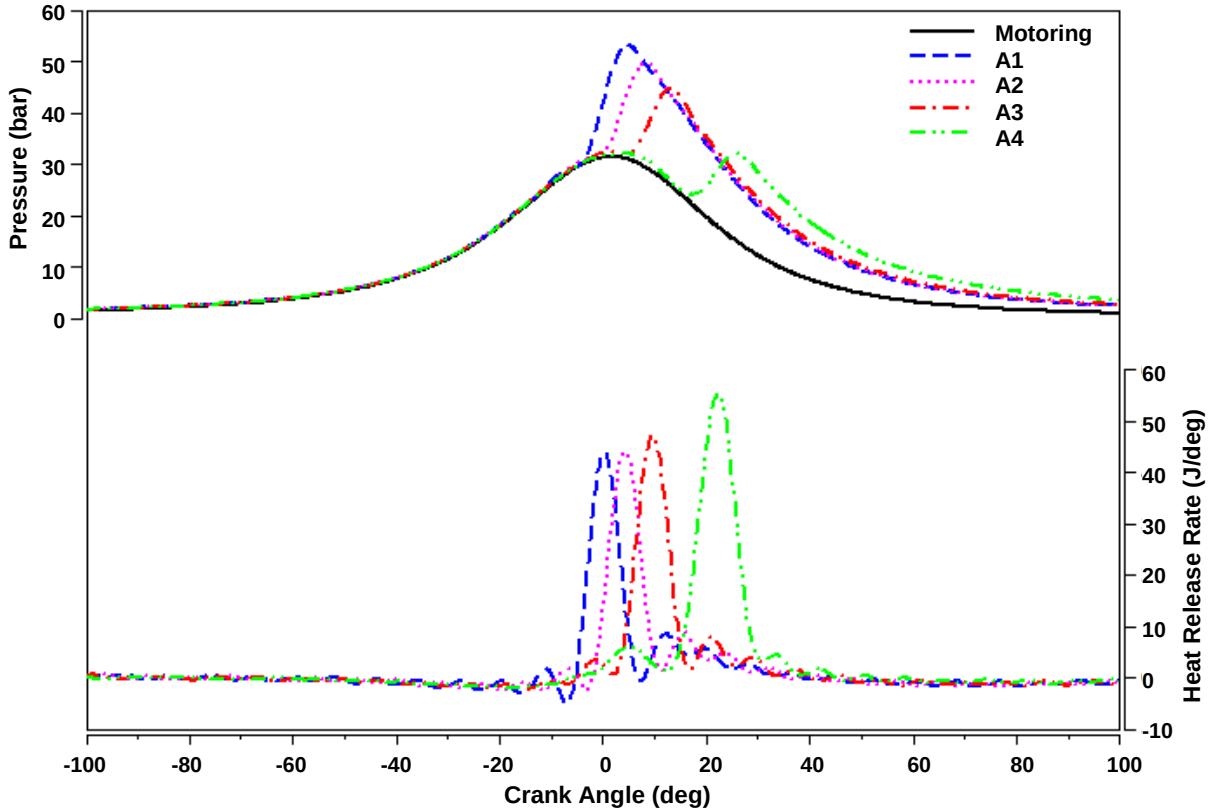

Figure 7. In-cylinder pressure and heat release rate for single injection strategies

The in-cylinder pressure and heat release rate data for the split injection strategies are depicted in Figure 8. As shown in this figure, when the split injection was employed, in-cylinder pressure and heat release rate curves exhibit different trends. The peak in-cylinder pressure first increased as the first injection was retarded from 20 to 15 CAD BTDC and then dropped slightly as the dwell angle was reduced to 10 CAD. The corresponding heat release curves showed that the heat release rate increased as the first injection timing was retarded, instead of remaining constant as with the single

injections. The split injection with 5 CAD dwell angle resulted in the highest peak in-cylinder pressure and heat release rate due to mainly the larger amount of fuel injected as the injector failed to close prior to the onset of the second injection, Figure 6. Therefore, the F4 strategy will not be discussed further.

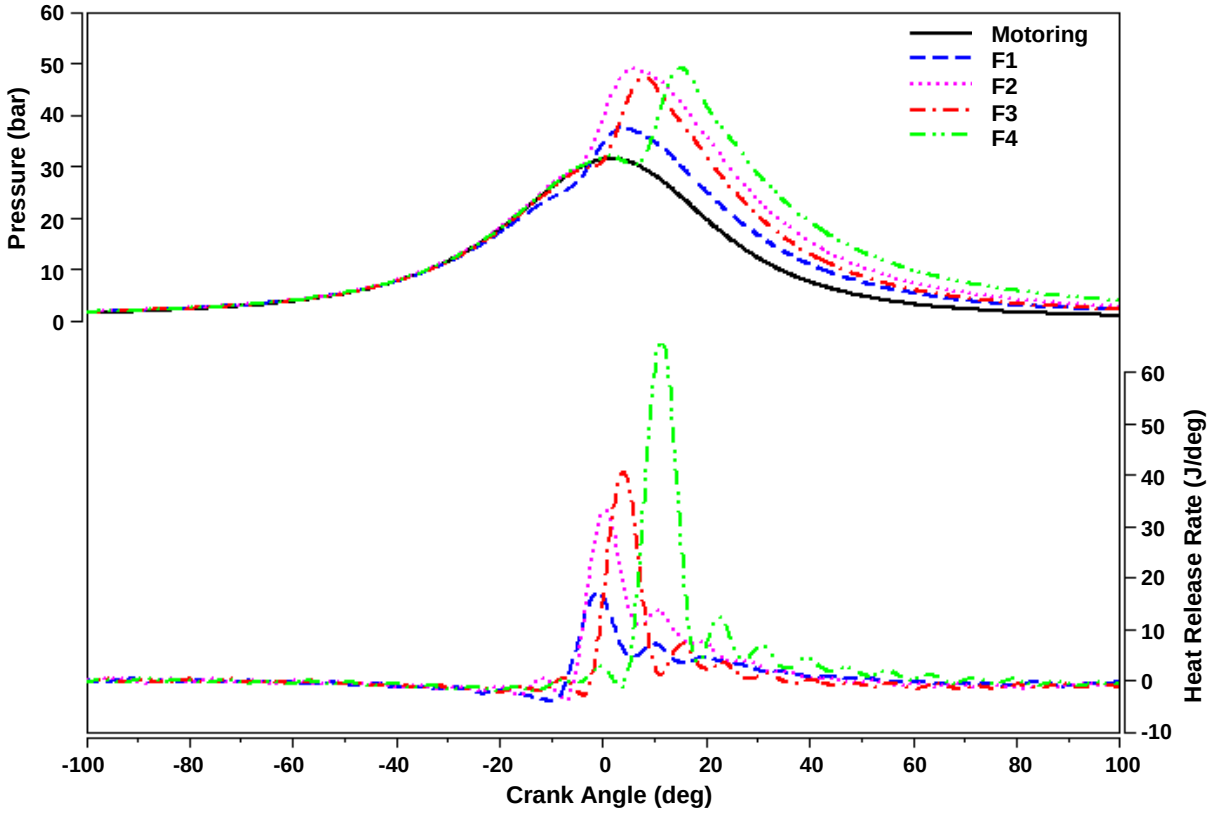

Figure 8. In-cylinder pressure and heat release rate for split injection strategies

The heat release rate curves exhibited a drop due to charge cooling effect shortly after the onset of the first fuel injection. Subsequently, the rate of heat release rapidly increased due to the premixed combustion. As given in Table 5, the ignition delay period decreased, due to improved fuel evaporation and mixing effects closer to TDC, as the injection timing was retarded. However, unlike the single injection strategies the percentage of combustion during the peak heat release period increased with shorter ignition delay associated with the retarded injection. In order to ascertain the primary causes of such a trend, high speed fuel spray and combustion visualisation technique was applied, Figure 9, in which the start of the first injection (SOFI), first visible combustion (FVC), start of the second injection (SOSI) and the maximum heat release rate (MHRR) for F1, F2 and F3 strategies were studied and compared. The high speed images obtained revealed that the increase in the percentage of combustion near and shortly after TDC during the peak heat release rate period was due to the interaction between the first and the second injections, whereby the fuel sprays during the second injection at TDC were injected into burning regions generated by the combustion of premixed fuel and air during the first injection. As a result, the premixed combustion of fuel from the first injection was intensified by the participation of the second injection. The effect of such interaction became more pronounced as the first injection timing was moved closer to TDC, Figure 9, where higher percentage of premixed combustion took place prior to the onset of the second fuel injection. From the results obtained, it is evident that the design limitations of the FIE as well as the possibility of interactions between the fuel injections during the combustion are amongst the complications that may be encountered in the application of split or multiple injection strategies. Therefore, thorough characterisation of the FIE and careful selection of injection strategies are essential for satisfactory implementation of such advanced injection modes.

The high speed fuel spray, combustion, flame temperature and soot distribution results obtained for the F2 strategy was selected for detailed analysis since the desired fuel quantity was injected for this strategy. The high speed image sequence for the F2 strategy is presented in Figure 10. The first four frames show the fuel spray jets development from the start to the end of the first injection where in the last frame, fuel sprays are almost fully evaporated. The fuel sprays in frames three and four are fully developed due to long injection duration of the first injection, 70% of total fuel quantity was injected at

this stage. The fuel spray impingement on the piston wall is evident from these images where the tip of the fuel sprays spread along the piston wall upon impact, generating a mushroom type structure. The first combustion phase which was apparent from the heat release rate data at -6.8 CAD ATDC, Figure 8, resulted in no visible combustion until -6.0 CAD ATDC where the first visible combustion was observed. The presence of relatively intense premixed combustion shortly after the end of the first fuel injection is evident at -5.1 CAD ATDC. The frames presented at TDC, 0.9 CAD ATDC (MHRR), 1.8 CAD ATDC and 3.6 CAD ATDC show the image sequence from the start to the end of the second injection. As previously stated, the fuel sprays during the second injection were injected into burning regions, generated by the combustion of premixed fuel and air shortly after the end of the first fuel injection. Consequently, autoignition took place vigorously at the tip of the fuel sprays during the second injection where fuel vapour was highly concentrated and spread along the periphery of the fuel sprays where fuel evaporation rate and its mixing with air were considerably higher as shown in frames

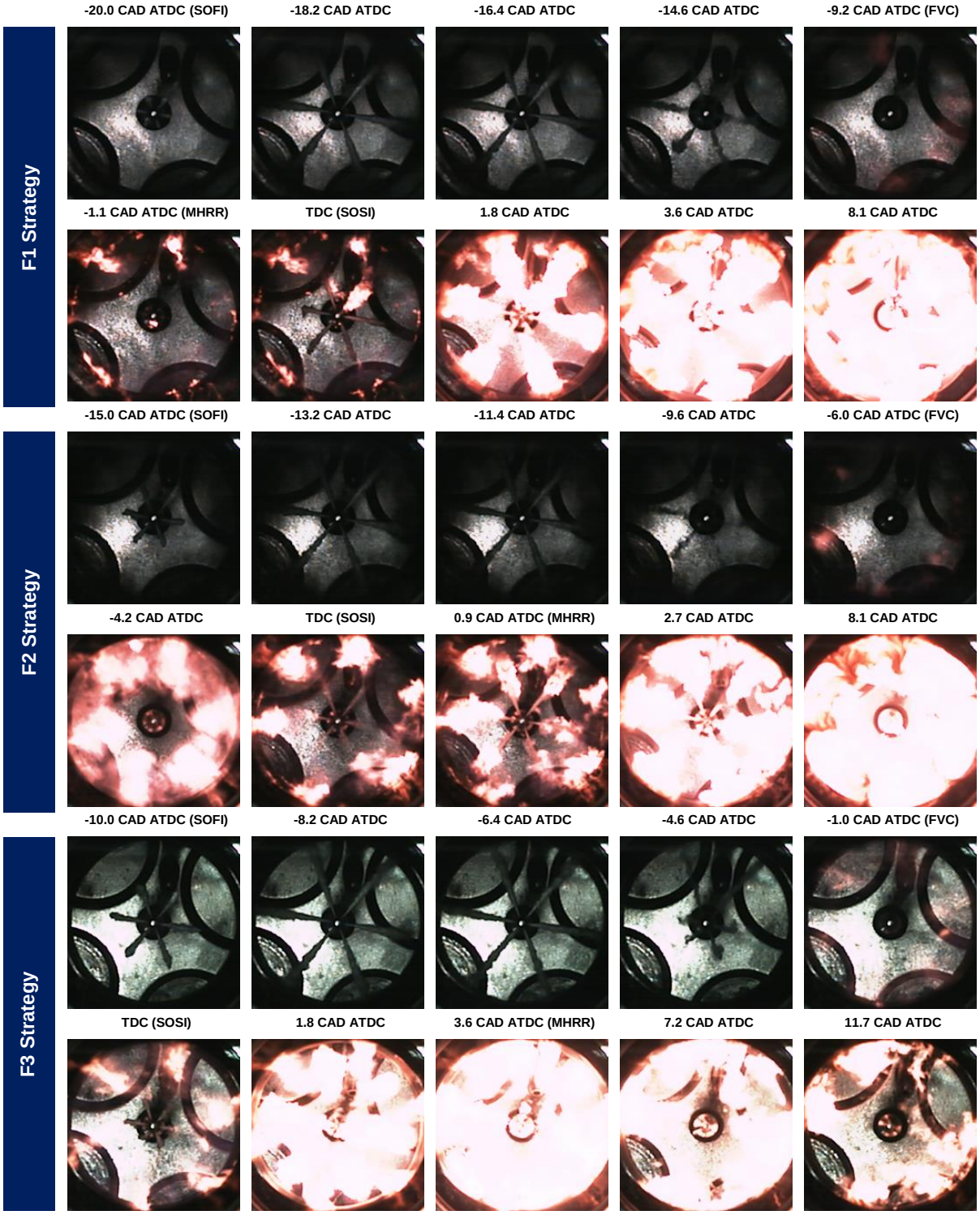

Figure 9. Combustion image sequence for split injection strategies

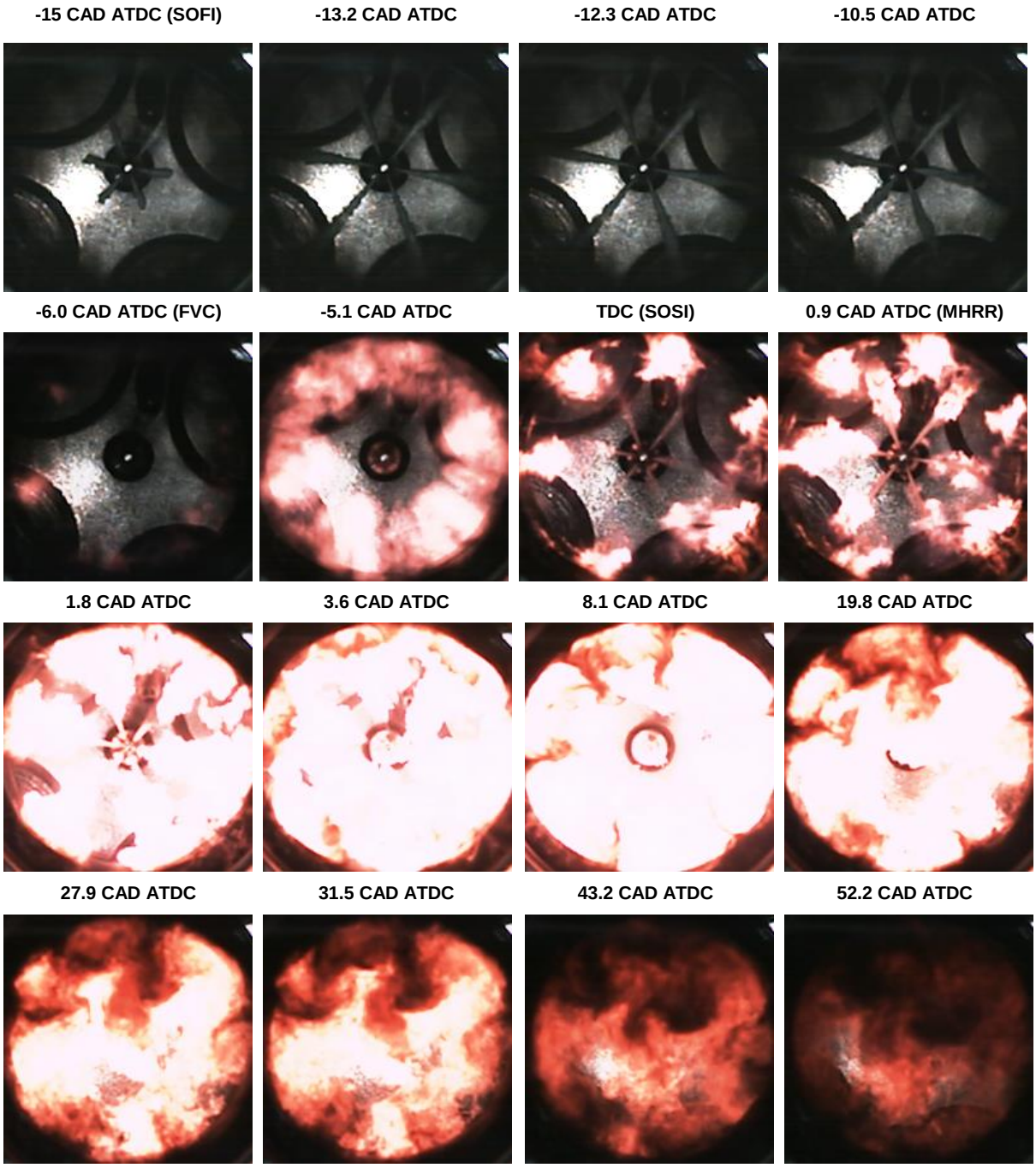

Figure 10. Combustion image sequence for F2 strategy

seven and eight at TDC and 0.9 CAD ATDC respectively. In the next frames at 1.8 CAD ATDC and 3.6 CAD ATDC, the autoignition combustion spread to the outer regions of the sprays tip due to the fuel sprays impingement on the piston wall, following the mushroom like structure previously created due to the fuel sprays impingement. In the subsequent frame at 8.1 CAD ATDC, burning region was fully expanded, covering the entire combustion chamber. The intense burning in these images indicated that substantial premixed and diffusion combustion took place for this strategy due to the interaction of the first and the second fuel injections, thus, high levels of NOx and soot emissions were expected. From the image sequence at 19.8 CAD ATDC, 27.9 CAD ATDC, 31.5 CAD ATDC, 43.2 ATDC and 52.2 CAD ATDC, it is evident that the flame intensity was diminishing during the expansion stroke and moving clockwise due to the swirl motion. Several combustion sites are present in these frames, indicating the presence of diffusion combustion corresponding to the second phase of combustion.

The flame temperature and KL factor image sequence for the F2 strategy are shown in Figure 11. Minor combustion at relatively low temperature was detected in the first frame at 0.9 CAD ATDC. The

subsequent frames at 1.8 CAD ATDC and 3.6 CAD ATDC showed combustion expansion around the tip and periphery of the sprays during the second fuel injection whereby fuel sprays were injected into burning regions. As the combustion process evolved, the gas temperature increased as evident in the next frame at 8.1 CAD ATDC where high temperature combustion was detected around the periphery of the piston bowl; this is in good agreement with the high speed image taken at this crank angle, Figure 10. As previously stated, the interaction between the first and the second fuel injections resulted in the occurrence of such rapid expansion of combustion. The flame temperature steadily decreased during the expansion stroke as shown in the image sequence at 19.8 CAD ATDC and 31.5 CAD ATDC respectively. Although luminous combustion was detected through high speed fuel spray and combustion imaging technique at crank angles before TDC and later in the expansion stroke, no information could be detected at these crank angles due to inadequate sensitivity of the detection system at the preselected wavelengths in this investigation (i.e. 550 nm and 750 nm). The intensifier gain could not be further increased due to image saturation at crank angles where highly luminous flame was present. Therefore, the first few frames at the initial and final stages of combustion were neglected.

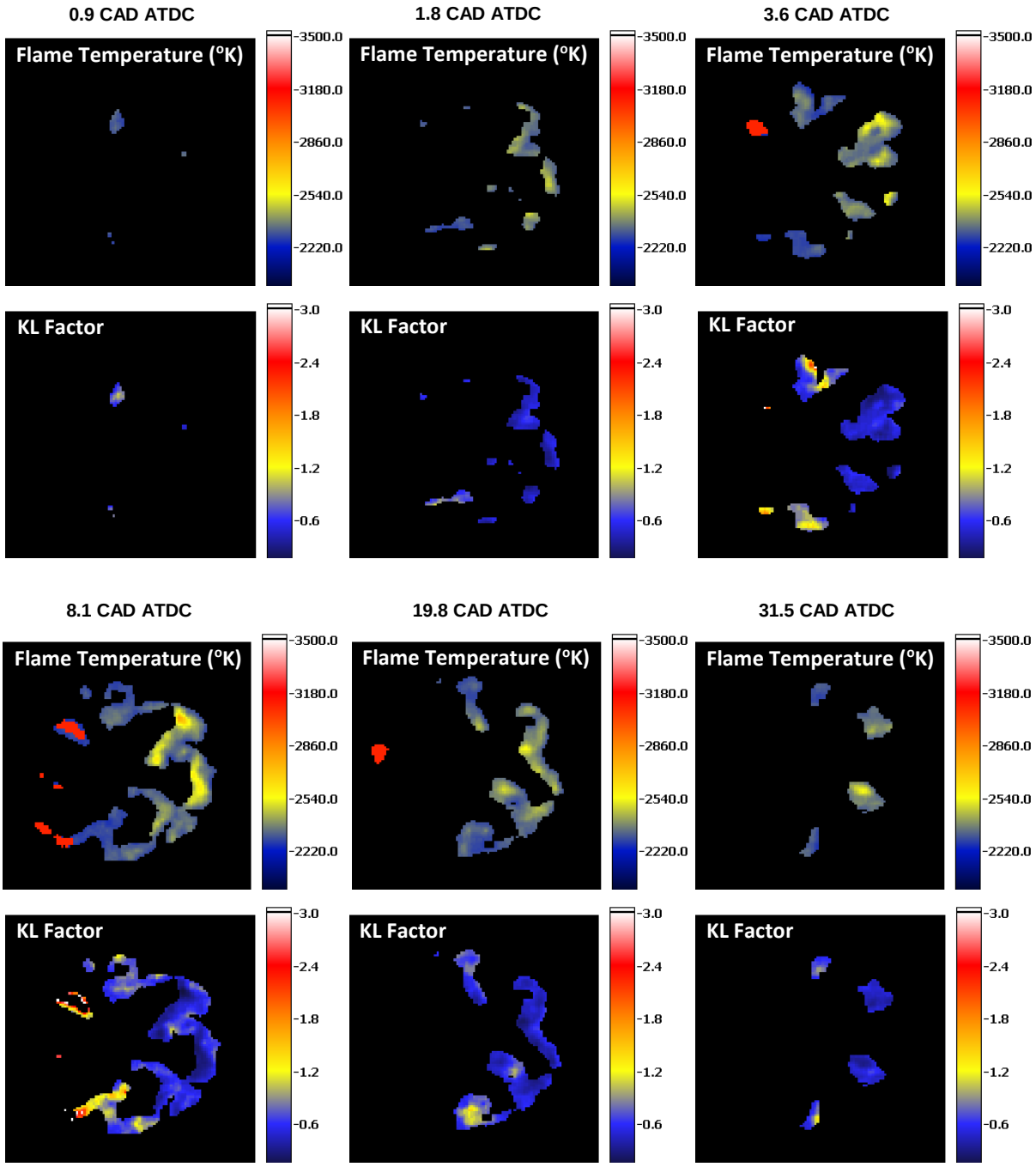

Figure 11. Flame temperature and KL factor image sequence for F2 strategy

The soot concentration distribution shown in Figure 11 followed the same pattern as those of the flame temperature image sequence as expected. As shown by the KL factor images at 0.9 CAD ATDC and 1.8 CAD ATDC, during initial stages of the combustion process, soot concentration was relatively low. The soot produced at this stage was due to the presence of combustion during the second fuel injection, leading to the rapid combustion of fuel vapour around the tip and the periphery of the fuel sprays during the second fuel injection process. In the next two frames at 3.6 CAD ATDC and 8.1 CAD ATDC, soot concentration increased spreading to the periphery of the piston bowl as the combustion process progressed during the expansion stroke. Soot was mainly concentrated around the tip of the fuel sprays and the periphery of the piston bowl where the gas temperature was considerably higher due to high concentration of fuel vapour. Soot concentration steadily decreased in the remaining image sequence mainly due to oxidation. The same explanation regarding low signal to noise ratio of the results holds true for the soot measurements. Therefore, although the trend in soot formation and oxidation could be determined, care must be taken in quantitative analysis of such results.

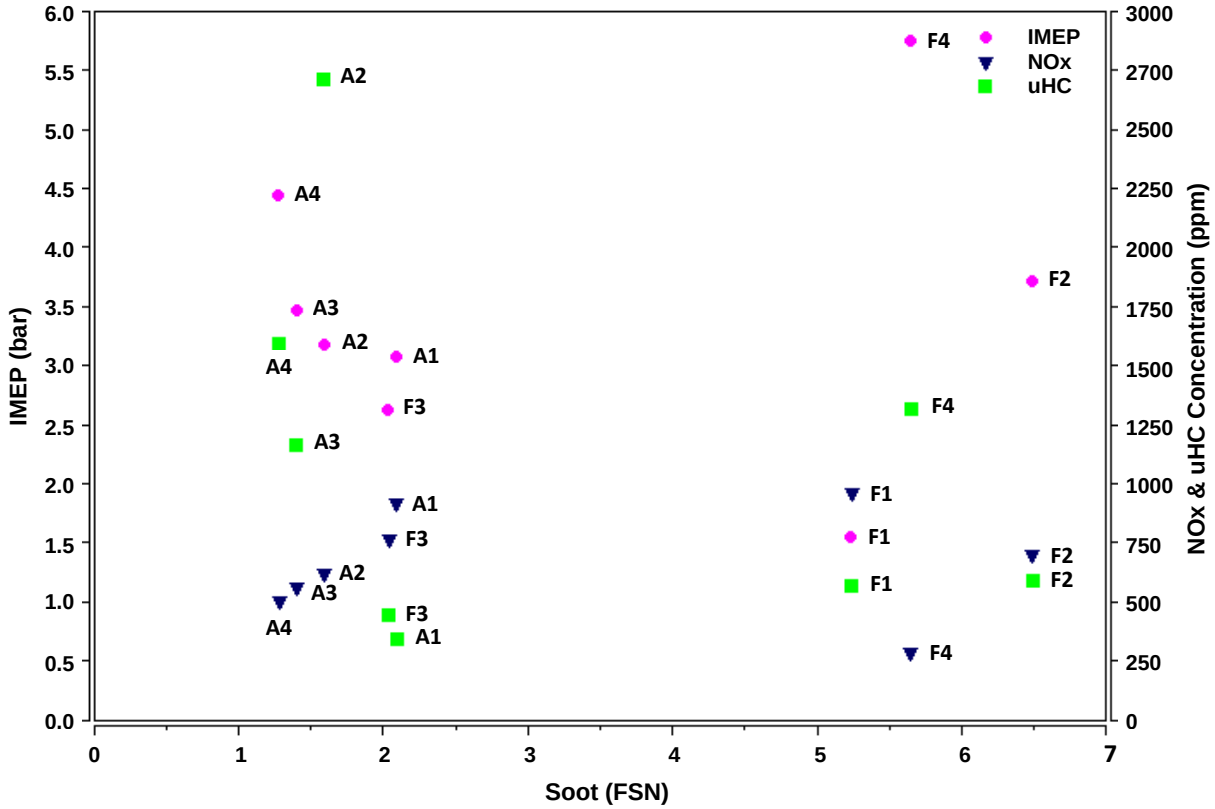

Figure 12. Engine output and emissions data for single and split injection strategies

The IMEP, soot, NOx and uHC emissions results are depicted in Figure 12. The substantial variations in the engine output and exhaust emissions for the investigated split injection strategies were primarily due to the inconsistency in the total fuel quantity injected as well as the interaction between the first and the second fuel injections. Nevertheless, F2 and A3 strategies can be compared since the total fuel quantity injected was almost identical. In comparison, F2 strategy resulted in higher IMEP value with considerably lower uHC, indicating improved fuel evaporation and mixing processes with significantly lower combustion noise. However, this injection strategy led to considerably higher soot and NOx emissions. The former was mainly attributed to the injection of fuel sprays into burning regions during the second injection, resulting in the propagation of highly luminous flame within the combustion chamber while the latter was due to the occurrence of relatively intense premixed combustion caused by the interaction between the two injections.

6 CONCLUSION

In this paper, the effects of dwell angle of split injection on the fuel injection system performance and in-cylinder mixture formation, combustion and soot distribution were investigated in a single cylinder CR fuel injection optical diesel engine. The fuel injection rate and interaction between two consecutive fuel injection events were quantified on a fuel injection characterisation rig. The in-cylinder process was studied by means of detailed heat release analysis and high speed optical imaging techniques.

The main findings can be summarised as follows: regarding the studied split injection strategies with variable dwell angle at 1200 bar injection pressure and the engine speed of 1500 rpm.

- Significant interactions were found between two closely spaced split injections in a solenoid CR fuel injector. Care must be taken to ensure that such interactions are considered and accounted for in advanced diesel combustion modes which require multiple injections.

- The in-cylinder high speed spray imaging and combustion visualisation techniques provided direct evidence of the interaction between combustion and fuel injection. The direct fuel injection into the premixed combustion from the first injection led to more pronounced heat release rate seen amongst the four cases studied.

- The results from the single and split injection strategies with similar total injected fuel quantities were compared, indicating the possibility of simultaneous improvement of engine performance and reduction of combustion noise. However, the tested split injection strategies resulted in higher soot emissions and almost similar NOx emissions.

Nevertheless, in order to identify the true effects of split injection with variable dwell angle on diesel combustion and emissions further detailed characterisation of the fuel injection system is required. In addition, an explicit conclusion on the advantages of split injection in comparison to that of conventional single injection can only be drawn provided that the effects of such phenomenon under various engine operating conditions are thoroughly assessed.

ACKNOWLEGMENT

The financial and technical support provided by Delphi Diesel Systems is gratefully acknowledged.

REFERENCES

1. European Automobile Manufacturers' Association, http://www.acea.be, (accessed 15 March 2010).
2. **Nehmer, D. A.** and **Reitz, R. D.** Measurement of the Effect of Injection Rate and Split Injections on Diesel Engine Soot and NOx Emissions, SAE paper 940668, 1994.
3. **Zambare, V. V.** and **Winterbone, D. E.** Photographic Investigation of Multi-Stage Fuel Injection in Single Cylinder DI Diesel Engine, SAE paper 1999-01-1501, 1999.
4. **Koyanagi, K., Öing, H., Renner, G.,** and **Maly, R.** Optimizing Common Rail-Injection by Optical Diagnostics in a Transparent Production Type Diesel Engine, SAE paper 1999-01-3646, 1999.
5. **Tanabe, K., Kohketsu, S.,** and **Nakayama, S.** Effect of Fuel Injection Rate Control on Reduction of Emissions and Fuel Consumption in a Heavy Duty DI Diesel Engine, SAE paper 2005-01-0907, 2005.
6. **Alriksson, M.** and **Denbratt, I.** Low Temperature Combustion in a Heavy Duty Diesel Engine Using High Levels of EGR, SAE paper 2006-01-0075, 2006.
7. **Zheng, M., Tan, Y., Mulenga, M. C.,** and **Wang, M.** Thermal Efficiency Analyses of Diesel Low Temperature Combustion Cycles, SAE paper 2007-01-4019, 2007.
8. **Dec, J. E.** Advanced Compression-Ignition Engines-Understanding the In-Cylinder Processes. *Proc. Combust. Inst.*, 2009, **32**(2), 2727-2742.
9. **Anselmi, P., Kashdan, J., Bression, G., Ferrero-Lesur, E., Thirouard, B.** and **Walter, B.** Improving Emissions, Noise and Fuel Economy Trade-Off by using Multiple Injection Strategies in Diesel Low Temperature Combustion (LTC) Mode, SAE paper 2010-01-2162, 2010.
10. **Knight, B. M., Bittle, J. A.,** and **Jacobs, T. J.** Characterizing the Influence of EGR and Fuel Pressure on the Emissions in Low Temperature Diesel Combustion, SAE paper 2011-01-1354, 2011.
11. **Caton J. A.** Thermodynamic Advantages of Low Temperature Combustion (LTC) Engines Using Low Heat Rejection (LHR) Concepts, SAE paper 2011-01-0312, 2011.
12. **Lu, X., Han, D.,** and **Huang, Z.** Fuel Design and Management for the Control of Advanced Compression-Ignition Combustion Modes. *Prog. Energy Combust. Sci.*, 2011, **37**(6), 741-783.
13. **Aceves, S. M., Flowers, D. L., Martinez-Frias, J., Smith, J. R., Dibble, R., Au, M.,** and **Girard, J.** HCCI Combustion: Analysis and Experiments, SAE paper 2001-01-2077, 2001.

14. **Wang, Z., Wang, J., Tian, G., Shuai, S., Zhang, Z.,** and **Yang, J.** Research on Steady and Transient Performance of an HCCI Engine with Gasoline Direct Injection, SAE paper 2008-01-1723, 2008.
15. **Yun, H., Wermuth, N.,** and **Najt, P.** High Load HCCI Operation Using Different Valving Strategies in a Naturally-Aspirated Gasoline HCCI Engine, SAE paper 2011-01-0899, 2011.
16. **Nevin, R. M., Sun, Y., Gonzalez, M. A.,** and **Reitz, R. D.** PCCI Investigation Using Variable Intake Valve Closing in a Heavy Duty Diesel Engine, SAE paper 2007-01-0903, 2007.
17. **Cao, L., Bhave, A., Su, H., Mosbach, S., Kraft, M., Dris, A.,** and **McDavid, R. M.** Influence of Injection Timing and Piston Bowl Geometry on PCCI Combustion and Emissions, SAE paper 2009-01-1102, 2009.
18. **Lu, Y., Yu, W.,** and **Su, W.** Using Multiple Injection Strategies in Diesel PCCI Combustion: Potential to Extend Engine Load, Improve Trade-off of Emissions and Efficiency, SAE paper 2011-01-1396, 2011.
19. **Park, Y.** and **Bae, C.** Influence of EGR and Pilot Injection on PCCI Combustion in a Single-Cylinder Diesel Engine, SAE paper 2011-01-1823, 2011.
20. **Benajes, J., Novella, R., Garcia, A., Domenech, V.,** and **Durrett, R.** An Investigation on Mixing and Auto-ignition using Diesel and Gasoline in a Direct-Injection Compression-Ignition Engine Operating in PCCI Combustion Conditions, SAE paper 2011-37-0008, 2011.
21. **Han, Z., Uludogan, A., Hampson, G. J.,** and **Reitz, R. D.** Mechanism of Soot and NOx Emission Reduction Using Multiple-Injection in a Diesel Engine, SAE paper 960633, 1996.
22. **Farrell, P. V., Chang, C. T.,** and **Su, T. F.** High Pressure Multiple Injection Spray Characteristics, SAE paper 960860, 1996.
23. **Zhang, Y., Ito, T.,** and **Nishida, K.** Characterization of Mixture Formation in Split-Injection Diesel Sprays via Laser Absorption-Scattering (LAS) Technique, SAE paper 2001-01-3498, 2001.
24. **Gill, K.** and **Zhao, H.** In-cylinder Studies of Fuel Injection and Combustion from a Narrow Cone Fuel Injector in a High Speed Single Cylinder Optical Engine, SAE paper 2008-01-1789, 2008.
25. **Ishikawa, S., Ohmori, Y., Fukushima, S., Suzuki, T., Takamura, A.,** and **Kamimoto, T.** Measurement of Rate of Multiple-Injection in CDI Diesel Engines, SAE paper 2000-01-1257, 2000.
26. **Zhao, H.** and **Ladommatos, N.** *Engine combustion instrumentation diagnostics*, 2001 (SAE International, Warrendale, Pennsylvania).
27. **Hottel, H. C.** and **Broughton, F. P.** The determination of true temperature and total radiation from luminous gas flames. *Ind. Engng Chem.*, 1932, **4**(2), 166-175.

APPENDIX

Notation

AFR	air-fuel ratio
ATDC	after top dead centre
CAD	crank angle degree
CMOS	complementary metal–oxide semiconductor
CN	cetane number
CR	common rail
CVC	constant volume chamber
FIE	fuel injection equipment
FSN	filter smoke number
FVC	first visible combustion
HCCI	homogenous charge compression ignition
HSDI	high-speed direct injection
IC	internal combustion
LAS	laser absorption scattering
LTC	low temperature combustion
MHRR	maximum heat release rate
NA	naturally aspirated
NOx	nitrogen oxides
PCCI	premixed charged compression ignition

PM	particulate matter
SOC	start of combustion
SOFI	start of first injection
SOSI	start of second injection
TDC	top dead centre
VCO	valve covered orifice